https://doi.org/10.30799/jnpr.118.25100201 J. Nat. Prod. Resour. - Volume 10 Issue 2 (2025) 309–315

Share Your Innovations through JACS Directory

Journal of Natural Products and Resources

Visit Journal at https://www.jacsdirectory.com/jnpr

ISSN: 2455-0299

Complete ^{1}H NMR Assignment of 3-Oxo-γ-Costic Acid from *Ageratina glabrata*

Antonio J. Oliveros-Ortiz, Jessica M. Lorenzo-García, Gabriela Rodríguez-García, Rosa E. del Río, Armando Talavera-Alemán, Mario A. Gómez-Hurtado*

Institute of Chemical-Biological Research, Building B-1, Michoacan University of Saint Nicholas of Hidalgo, Univ. City, Morelia, Michoacán 58030, Mexico.

ARTICLE DETAILS

Article history:
Received 22 September 2025
Accepted 09 October 2025
Available online 17 October 2025

Keywords:
NMR Assignment
3-Oxo-γ-Costic Acid
Eudesmene Sesquiterpene
DFT

ABSTRACT

Nuclear Magnetic Resonance (NMR) is a powerful technique for elucidating the structure of organic molecules, and it is especially useful in determining the structure of natural products, including terpenes. 3-Oxo-γ-costic acid is an eudesmene-type sesquiterpene that has been isolated from different vegetable species of the Asteraceae and Lauraceae families. Its ^{1}H NMR has been reported with some discrepancies in the chemical shift assignments as well as in *J* values. In the present work, 3-oxo-γ-costic acid was isolated from the dichloromethane extract of the aerial parts of *Ageratina glabrata* by chromatographic means and the complete assignment of the ^{1}H NMR spectrum of 3-oxo-γ-costic acid is reported using a hybrid protocol that involves a DFT-calculated spectrum and the experimental ^{1}H spectrum. The calculated spectrum was constructed based on the DFT-calculated *J* values for each hydrogen, and the respective chemical shifts are those recorded by experimental means, which are supported by 2D NMR. Then, the completely calculated ^{1}H spectrum was simulated in the Mnova software and compared with the experimental spectrum. This methodology is especially useful for the detection of low magnitude NMR couplings (<2 Hz), which are complicated to measure experimentally; then, this hybrid protocol, experimental-DFT, could be applied to NMR determination of more complex sesquiterpenes.

1. Introduction

Nuclear Magnetic Resonance technique provides information about functional groups, stereochemistry, and conformational preferences [1-3]. ^{1}H NMR determination in natural products, especially in terpenes, presents a challenge due to the complexity of their spectra, which typically exhibit intricate patterns that complicate the determination of multiplicities and *J* values. That spectral complexity also provides additional information on chemical microenvironments and spatial relationships [4,5]. In this context, quantum mechanics calculations and computational tools play an essential role in multi-spin system simulation, chemical shifts optimization, and the determination of coupling constant values, which allows confident assignment by comparison of the experimental spectra with those obtained by theoretical calculations [4,6-9]. 3-Oxo-γ-costic acid is an eudesmene-type sesquiterpene isolated from different plant species, including *Ageratina glabrata* [10], *Artemisia altaiensis* [11], *Crepis sancta* [12], *Chiliadenus montanus* [13], *Tessaria absinthioides* [14], and *Nectandra cissiflora* [15]. This compound has demonstrated biological activities as antibacterial [16], allelochemical effect against *Tribolium castaneum* [14], moderate cytotoxic activity against mouse lymphoma (L5178Y) cells [12], as well as antiproliferative activity against colorectal adenocarcinoma Caco-2 cells [17]. Its structural elucidation has been achieved by NMR means, including ^{1}H and ^{13}C spectra, while the absolute configuration was reported by monocrystal X-ray diffraction in 1998 [11]. Although reports on its ^{1}H spectrum exist [10,12,15-17], discrepancies remain in the chemical shift assignments as well as the reported *J* values, particularly in the low-frequency region where the signals overlap. In the present work, the complete assignment of the ^{1}H NMR spectrum of 3-oxo-γ-costic acid, isolated from *Ageratina glabrata*, was established by comparison of the experimental spectra with the data obtained by DFT-B3LYP/6-31G(d,p) uþ1s calculations. This work contributes to the literature on the complete assignment of the ^{1}H NMR spectrum of this eudesmane sesquiterpenoid and suggests an applicable methodology for the characterization of other natural products of chemical and biological interest.

2. Experimental Methods

2.1 General Procedures

Solvents were distilled prior to their use. The melting point was determined using a Fisher-Johns apparatus and is uncorrected. ^{1}H, ^{13}C NMR, and 2D NMR spectra were recorded in a Varian Mercury Plus 400 spectrometer. The solvent was $CDCl_3$, and TMS served as the internal reference. Chemical shift values (δ) are reported in parts per million, and coupling constants (*J*) are given in Hz. NMR spectra were processed using the Mnova software.

2.2 Plant Material

Specimens of *Ageratina glabrata* were collected near km 4.5 of Pátzcuaro-Santa Clara del Cobre federal road, Michoacán State, México (N 19°29.516′ W 101°35.273′). A specimen was deposited (voucher no. 226133) at the Herbarium of the Instituto de Ecología, A.C., Centro Regional del Bajío, Pátzcuaro, Michoacán, Mexico.

2.3 Extraction and Isolation of 3-Oxo-γ-Costic Acid

3-Oxo-γ-costic acid was isolated from aerial parts of *Ageratina glabrata* following the phytochemical march as previously reported [10]. Colorless crystals, m.p. 155-157 °C Lit. 153 °C [10]. ^{1}H NMR at 400 MHz in $CDCl_3$, (Table 1). ^{13}C NMR (100 MHz in $CDCl_3$) agreed with data described (see Appendix) [16]. 2D NMR spectra are provided in Appendix (A3-A5).

2.4 ^{1}H NMR Spin-Spin Analysis of 3-Oxo-γ-Costic Acid

A molecular model of 3-oxo-γ-costic acid was constructed in silico and subjected to the Monte Carlo protocol using Merck Molecular Force Field (MMFF94) within an energy window of 0-5 kcal/mol. A total of 13 conformers were obtained and then subjected to a geometry optimization using the DFT B3LYP/6-31G (d,p) level of theory in the Gaussian 16 software. From this, the nine conformers within a gap energy of 0-3 kcal/mol were obtained. The *J* values were calculated for each conformer at the DFT B3LYP/6-31G(d,p) uþ1s level of theory [18], and the Boltzmann-averaged data were used to compare with the experimental ^{1}H spectrum. The calculated *J* values were analyzed using the SpinWorks 4 program (Version 4.2.12.0), considering individual spin systems up to 8, according to the limitations of the software, with a maximum of 30

*Corresponding Author:mario.gomez@umich.mx(Mario A. Gómez-Hurtado)

https://doi.org/10.30799/jnpr.118.25100201

Cite this Article as: Antonio J. Oliveros-Ortiz, Jessica M. Lorenzo-García, Gabriela Rodríguez-García, Rosa E. del Río, Armando Talavera-Alemán, Mario A. Gómez-Hurtado, Complete ^{1}H NMR assignment of 3-oxo-γ-costic acid from *Ageratina glabrata*, J. Nat. Prod. Resour. 10(2) (2025) 309-315.

iterations, RMSD convergence of 0.200, and RMS for auto-assign of 0.1000. Spin simulation using the SpinWorks software, with iterative adjustments of δ and *J* values, allowed the isolation of the signals theoretically obtained. The chemical shift values to construct the calculated ^{1}H spectrum were assigned based on the experimental ^{1}H data using the HETCOR experiment as the reference (Appendix A4). Finally, a calculated ^{1}H NMR spectrum was constructed using the Mnova software (Version 14.2.3-29241) using the prediction module with the spin simulation tool, considering a system of 15 different spins, and compared with the experimental. Computational calculations were performed using a CPU ES-2680 v3 with 110 GB of RAM, operating at 2.5 GHz with 48 core processors.

3. Results and Discussion

Herein, 1D and 2D NMR experiments for 3-oxo-γ-costic acid were determined (see Appendix), which enabled the establishment of its chemical structure (Fig. 1). Several studies on the isolation and characterization of this sesquiterpene have been described [10,12,15-17]. In those reports, several variations were highlighted when comparing the ^{1}H NMR data, including a lack of multiplicities and *J* values. The experimental ^{1}H NMR spectrum of 3-oxo-γ-costic acid (400 MHz in $CDCl_3$) displayed the expected signal pattern, including the vinyl protons H13a and H13b at δ 6.42 and 5.76, respectively, the allylic methylene protons CH_2-6 appeared at δ 2.88 and 2.05, the methyl protons CH_3-14 and CH_3-15 at δ 1.78 and 1.25, as well as highly overlapped signals, particularly at δ 2.67 - 2.30 and at δ 1.90-1.65 ranges. The direct interpretation of those highly populated regions proved ineffective for establishing a precise multiplicity assignment, but chemical shifts were secured by analyzing the HETCOR experiment. Thus, computational tools, including Mnova and SpinWorks, as well as Density Functional Theory (DFT) calculations, were employed to elucidate the complete ^{1}H assignments for 3-oxo-γ-costic acid (Fig. 2). These programs have been demonstrated to be key tools for NMR data analysis [19-21].

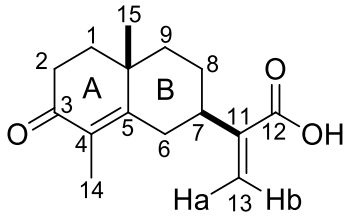

Fig. 1 Structure of 3-oxo-γ-costic acid

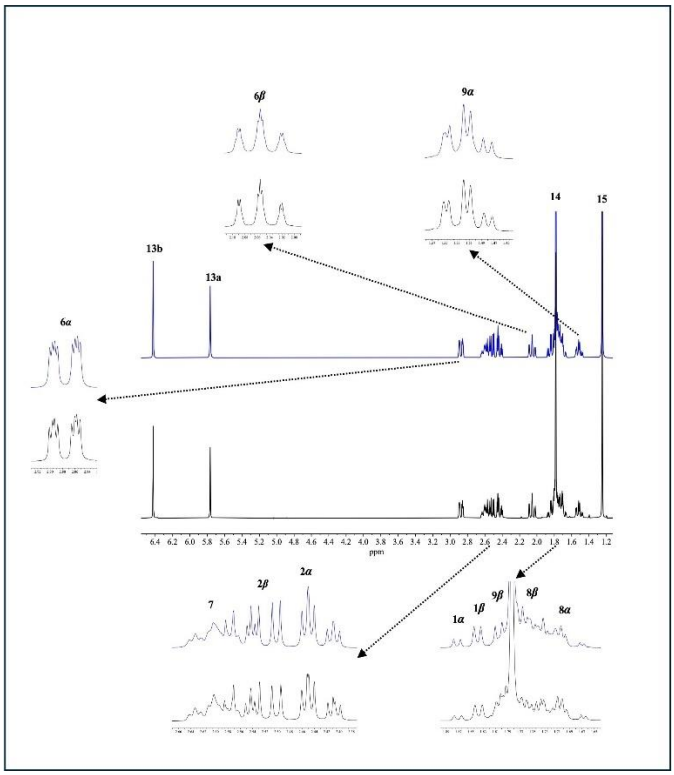

Fig. 2 Calculated (blue) and experimental (black) ^{1}H NMR spectra of 3-oxo-γ-costic acid in $CDCl_3$ at 400 MHz

It follows that the calculated ^{1}H NMR spectrum of 3-oxo-γ-costic acid was pursued. A molecular model of 3-oxo-γ-costic acid was built, and its conformational distribution was explored using the Monte Carlo protocol. An energy gap of 0–5 kcal/mol was established as the conformer cutoff, providing 13 conformers. After, energy optimization of the whole conformers was achieved by density functional theory (DFT) at the B3LYP/6-31G(d), and those in the 0-3 kcal/mol energy window were used to calculate their respective theoretical *J* values using DFT B3LYP/6-31G(d,p) uþ1s level of theory. These data were calculated following the Bally and Rablen protocol [18], which combines geometry optimization (B3LYP/6-31G(d)) with the calculation of Fermi contact terms and an empirical scale correction (~0.9155). The Boltzmann-averaged data were analyzed to establish the final *J* values and are listed in Table 1. After, the *J* values obtained were supported by spin simulations using the SpinWorks program. Finally, the *J* values were uploaded into the Mnova Program to get the whole simulated ^{1}H spectra as observed in Fig. 2.

Protons H-13a and H-13b are typically described without defined couplings and fall within the ranges of δ 5.28-5.76 and 6.34-6.41 [10,15]. Herein, we established the H-13a and H-13b resonances as a doublet each (*J* = 0.65 Hz) at δ 5.766 and 6.423. Methyl groups CH_3-14 and CH_3-15 (δ 1.25) were previously described as singlets; however, spin-spin simulation and DFT validation suggested that CH_3-14 (δ 1.784) displayed long-distance coupling of *J* = 1.60 Hz with H-6*α*. This type of coupling has been previously evidenced through the analysis of methyl motifs at the H−Csp^3 −Csp^2 = Csp^2 dihedral angle (θ) level from aromatic compounds [22], thus suggesting planarity in this section of the molecule. Notwithstanding, the B ring revealed a chair conformational preference, as is didactically illustrated in Fig. 3, by the measured dihedrals in the global minimum conformer. By its part, ring A revealed a half-chair conformational preference.

According to our results, H-6*α* resonance is assigned at δ 2.876 as double of doublets of quadruplets (*J* = −14.70, 3.40, 1.60), while H-6*β* is observed at δ 2.056 as double of doublets of doublets (*J* = −14.70, 13.10, 2.00). In this case, the H-6α proton can be electronically influenced by the α,β-unsaturated ketone motif, thereby resulting in a chemical shift at significantly higher frequencies compared to H-6*β* [23]. The H-7 resonance was observed at δ 2.602 (dddd, *J* = 13.10, 12.17, 3.50, 3.40). According to these results, notable discrepancies were detected concerning previous reports. While Bohlmann et al [10] reported CH_2-6 and CH-7 resonances as doublets of doublets each, Garcez and coworkers [15] described H-6α as a doublet, H-6*β* as a triplet, and H-7 as a multiplet signal.

Table 1. ^{1}H chemical shifts (ppm), coupling orders, and coupling constants (Hz) of 3-oxo-γ-costic acid

H	δ ^{1}H	*J* in Hz
1*α*	1.836	$^2J_{1\alpha,1\beta}$ = −13.08, $^3J_{1\alpha,2\beta}$ = 14.69, $^3J_{1\alpha,2\alpha}$ = 4.08
1*β*	1.764	$^2J_{1\beta,1\alpha}$ = −13.08, $^3J_{1\beta,2\beta}$ = 4.63, $^3J_{1\beta,2\alpha}$ = 3.53
2*α*	2.434	$^2J_{2\alpha,2\beta}$ = −16.40, $^3J_{2\alpha,1\alpha}$ = 4.08, $^3J_{2\alpha,1\beta}$ = 3.53
2*β*	2.535	$^2J_{2\beta,2\alpha}$ = −16.40, $^3J_{2\beta,1\alpha}$ = 14.69, $^3J_{2\beta,1\beta}$ = 4.63
6*α*	2.876	$^2J_{6\alpha,6\beta}$ = −14.70, $^3J_{6\alpha,7}$ = 3.40, $^4J_{6\alpha,14}$ = 1.60
6*β*	2.056	$^2J_{6\beta,6\alpha}$ = −14.70, $^3J_{6\beta,7}$ = 13.10, $^5J_{6\beta,8\alpha}$ = 2.00
7	2.602	$^3J_{7,6\beta}$ = 13.10, $^3J_{7,8\beta}$ = 12.17, $^3J_{7,8\alpha}$ = 3.50, $^3J_{7,6\alpha}$ = 3.40
8*α*	1.719	$^2J_{8\alpha,8\beta}$ = −13.22, $^3J_{8\alpha,9\alpha}$ = 3.91, $^3J_{8\alpha,7}$ = 3.50, $^3J_{8\alpha,9\beta}$ = 2.85, $^4J_{8\alpha,6\beta}$ = 2.00
8*β*	1.778	$^2J_{8\beta,8\alpha}$ = −13.22, $^3J_{8\beta,9\alpha}$ = 13.56, $^3J_{8\beta,7}$ = 12.17, $^3J_{8\beta,9\beta}$ = 3.65
9*α*	1.516	$^2J_{9\alpha,9\beta}$ = −13.00, $^3J_{9\alpha,8\beta}$ = 13.56, $^3J_{9\alpha,8\alpha}$ = 3.91
9*β*	1.729	$^2J_{9\beta,9\alpha}$ = −13.00, $^3J_{9\beta,8\beta}$ = 3.65, $^3J_{9\beta,8\alpha}$ = 2.85
13a	5.766	$^2J_{13a,13b}$ = 0.65
13b	6.423	$^2J_{13b,13a}$ = 0.65
14	1.784	$^5J_{14,6\alpha}$ = 1.60

The signals in the δ 2.6-1.6 range presented an interesting challenge due to the overlapping signal levels. Decomposition in spin systems using SpinWorks, with iterative adjustments of δ and *J* values, allowed us to isolate the signals theoretically and model the complex couplings predicted by DFT using the SpinWorks and Mnova programs. It follows that the methodology allows for the precise assignment of protons H-1*α* and H-1*β* at δ 1.836 (ddd, *J* = −13.08, 14.69, 4.08 Hz) and δ 1.764 (ddd, *J* = −13.08, 4.63, 3.53 Hz), respectively. On the other hand, H-2*β* was shifted to δ 2.535 (ddd, *J* = −16.40, 14.69, 4.63 Hz) and H-2*α* was found at δ 2.434 (ddd, *J* = −16.40, 4.08, 3.53 Hz). The geminal coupling value (*J* = −16.40 Hz) and vicinal couplings are directly related to the rigid geometry of the bicyclic skeleton [24]. In this range, H-9*β* (δ 1.729), H-8*β* (δ 1.778), and H-8*α* (δ 1.719) signals were also assigned. Vicinal coupling of H-9*β* with H-8*β*, and H-8*α* (*J* = 3.65 and 2.85 Hz, respectively), as well as geminal coupling (*J* = −13.00 Hz) was determined. The H-8*β* proton revealed a higher level of coupling as expected, including geminal (*J* = −13.22 Hz), vicinal H-8*β*/H-7 (*J* = 12.17 Hz), H-8*β*/H-9*α* (*J* = 13.56 Hz), and H-8*β*/H-9*β* (*J* = 3.65 Hz) couplings. In addition to the above-mentioned *J* couplings related to H-8*α*, this proton also revealed the vicinal coupling H-8*α*/H-7 (*J*

https://doi.org/10.30799/jnpr.118.25100201

= 3.50 Hz) and H-8α/H-9α (J = 3.91 Hz), as well as the W-type coupling H-8α/H-6β (J = 2.00 Hz). Finally, H-9α resonance was observed at δ 1.516 with the expected couplings with H-9β, H-8β, and H-8α.

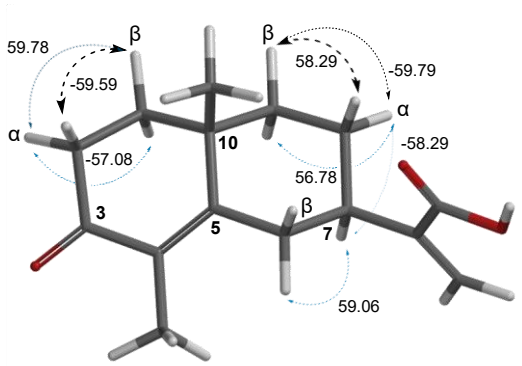

Fig. 3 Global minimum conformer obtained at the DFT B3LYP/6-31G(d,p) level of theory. Calculated dihedrals are depicted in the figure in degrees as follows: H1α-C1-C2-H2α; H1β-C1-C2-H2α; H1β-C1-C2-H2β; H7-C7-C6-H6α; H7-C7-C8-H8α; H9α-C9-C8-H8α; H9β-C9-C8-H8α. In addition, measured *trans*-diaxial dihedrals are: H1α-C1-C2-H2β = −176.45°; H7-C7-C6-H6β = 174.59°; H7-C7-C8-H8β = −175.27°; H9α-C9-C8-H8β = 174.85°

4. Conclusion

The complete assignment of the ^{1}H NMR spectrum of the 3-oxo-γ-costic acid was established by comparison of both the experimental and the simulated spectra. The hybrid protocol included the Gaussian, SpinWorks, and Mnova programs. According to the results, this methodology could be applied as an alternative to ^{1}H NMR assignment of terpenoid compounds in a facile and computationally economical manner. This methodology proved to be especially useful for the detection of low-magnitude NMR couplings (<2 Hz), which are challenging to measure experimentally. This analysis avoids speculations in assignments and offers a reproducible methodology that could become a routine in advanced structural elucidation. Also, the integration of experimental NMR, together with simulation tools and quantum chemical validation, could overcome limitations inherent to experimentation, such as the resolution of magnetically equivalent protons or the overlap in the aliphatic region of the spectra.

Author Contributions

Antonio J. Oliveros-Ortiz: Investigation, Methodology, Experiments, Data Analysis; *Jessica M. Lorenzo-García:* Investigation, Experiments; *Gabriela Rodríguez-García:* Investigation, Data Curation, Formal Analysis, Writing–Review and Editing; *Rosa E. del Río*: Supervision, Data Curation, Formal Analysis, Writing–Review and Editing; *Armando Talavera-Alemán*: Conceptualization, Formal Analysis, Writing–Review and Editing; *Mario A. Gómez-Hurtado*: Conceptualization, Writing – Original Draft. All authors have read and agreed to the published version of the manuscript.

Funding

CIC-UMSNH funded this research

Competing Interests

The authors declare that they have no competing interests.

Acknowledgement

A.J.O.O. and J.M.L.G. are grateful to SECIHTI-Mexico for scholarships 800679 and 828930, respectively. Authors also thank Pedro Navarro-Santos for technical support.

References

[1] C. Li, Y. Cong, W. Deng, Identifying molecular functional groups of organic compounds by deep learning of NMR data, Magn. Reson. Chem. 60 (2022) 1061-1069.
[2] X. Li, X. Yang, H. Sun, NMR for stereochemical elucidation, in: Q.B. Cass, M.E. Tiritan, J.M.B. Junior, J.C. Barreiro, (Eds.), Chiral separations and stereochemical elucidation: Fundamentals, methods, and applications, John Wiley & Sons Ltd, USA, 2023, pp.505-549.
[3] Y.H. Kim, S.Y. Lee, J.Y. Kim, H. Cho, H.S. Chun, S. Ahn, Nuclear magnetic resonance-based approaches for the structural and quantitative analysis of mycotoxins, Magnetochemistry 11 (2025) 47.
[4] L. Botros, Y. Liu, C. Corbett, D. Sørensen, C. Szabo, A. Bzhelyansky, M. Niemitz, P. Korhonen, G.F. Pauli, P. Giraudeau, G.J. Ray, Connecting the practice of modern qualitative and quantitative NMR analysis with its theoretical foundation, J. Nat. Prod. 88 (2025) 877–888.
[5] J.C. Pardo-Novoa, C.M. Cerda-García-Rojas, C. New techniques of structure elucidation for sesquiterpenes, in: A.D. Kinghorn, H. Falk, S. Gibbons, J. Kobayashi, Y. Asakawa, J.-K. Liu, (Eds.), Progress in the Chemistry of Organic Natural Products, Vol. 114, Springer, Cham., 2021, pp. 253-311.
[6] M. Niklasson, R. Otten, A. Ahlner, C. Andresen, J. Schlagnitweit, K. Petzold, P. Lundström, Comprehensive analysis of NMR data using advanced line shape fitting, J. Biomol. NMR. 69 (2017) 93-99.
[7] S.B. Paudel, J.W. Nam, G.G.R. Malca, B. Shapiro, P. Laatikainen, Y. Liu, A digital platform for automated analysis of ^{1}H NMR data: prototype framework of digital reference standard, AAPS Open 11 (2025) 2.
[8] C. Feng, E.L. Kovrigin, C.B. Post, NmrLineGuru: standalone and user-friendly GUIs for fast 1D NMR lineshape simulation and analysis of multi-state equilibrium binding models, Sci. Rep. 9 (2019) 16023.
[9] D.A. Cheshkov, K.F. Sheberstov, D.O. Sinitsyn, V.A. Chertkov, ANATOLIA: NMR software for spectral analysis of total lineshape, Magn. Reson. Chem. 56 (2017) 449-457.
[10] F. Bohlmann, J. Jakupovic, M. Lonitz, Natürlich vorkommende Terpen-derivate, 76. Über Inhaltsstoffe der Eupatorium-Gruppe, Chem. Ber. 110 (1977) 301-314.
[11] M.A. Khanina, A.T. Kulyyasov, I.Y. Bagryanskaya, Y.V. Gatilov, S.M. Adekenov, V.A. Raldugin, 3-Oxocostusic acid from *Artemisia altaiensis*, Chem. Nat. Compd. 34 (1998) 145-147.
[12] S.S. Ebada, N.A. Al-Jawabri, F.S. Youssef, A. Albohy, S.M. Aldalaien, A.M. Disi, P. Proksch, *In vivo* antiulcer activity, phytochemical exploration, and molecular modelling of the polyphenolic-rich fraction of *Crepis sancta* extract, Inflammopharmacology 28 (2020) 321-331.
[13] M.E.F. Hegazy, H. Matsuda, S. Nakamura, T.A. Hussein, M. Yoshikawa, P.W. Paré, Chemical constituents and their antibacterial and antifungal activity from the Egyptian herbal medicine *Chiliadenus montanus*, J. Phytochem. 103 (2014) 154–161.
[14] M. García, M. Sosa, O.J. Donadel, O.S. Giordano, C.E. Tonn, Allelochemical effects of eudesmane and eremophilane sesquiterpenes on *Tribolium castaneum* larvae, J. Chem. Ecol. 29 (2003) 175-187.
[15] F.R. Garcez, W.S. Garcez, L. Hamerski, A.C.M. Miranda, Eudesmane and rearranged eudesmane sesquiterpenes from *Nectandra cissiflora*, Quím. Nova 33 (2010) 1739-1742.
[16] M.M. Al-Dabbas, F. Hashinaga, S.A.M. Abdelgaleil, T. Suganuma, K. Akiyama, H. Hayashi, Antibacterial activity of an eudesmane sesquiterpene isolated from common *Varthemia*, *Varthemia iphionoides*, J. Ethnopharmacol. 97 (2005) 237-240.
[17] M.E.F. Hegazy, A. Ahmed, A.R. Hamed, A.A.A. Elaty, N.S. Mohamed, P.W. Pare, 3-Oxo-γ-costic acid fungal-transformation generates eudesmane sesquiterpenes with in vitro tumor-inhibitory activity, Bioorg. Med. Chem. Lett. 27 (2017) 3825-3828.
[18] T. Bally, P.R. Rablen, Quantum-Chemical simulation of ^{1}H NMR spectra. 2. Comparison of DFT-based procedures for computing proton–proton coupling constants in organic molecules, J. Org. Chem. 76 (2011) 4818-4830.
[19] M.R. Willcott, MestReNova (Computer Software Review), J. Am. Chem. Soc. 131 (2009) 13180-13180.
[20] M. Edgar, D. Hayward, F. Zeinali, S. Riaz, G.W. Weaver, NMR spectral analysis of strongly second-order 6-, 8-, 9- and 10- spin-systems (^{1}H—^{19}F, ^{19}F—^{19}F, and ^{13}C—^{19}F) in perfluorotoluyl- and tetrafluoro-pyridyl-aromatics using the lineshape method ANATOLIA. Magn. Reson. Chem. 58 (2020) 170–185.
[21] L.B. Krivdin, Computational ^{1}H and ^{13}C NMR in structural and stereochemical studies, Magn. Reson. Chem. 60 (2022) 733-828.
[22] N. Pérez-Hernández, C. Álvarez-Cisneros, C. M. Cerda-García-Rojas, M. S. Morales-Ríos, P. Joseph-Nathan, Benzylic coupling constants in toluene derivatives by J doubling in the frequency domain and DFT calculations, Magn. Reson. Chem. 47 (2009) 437-442.
[23] H. Dodziuk, Non-bonded interactions, and the allylic and anomeric effects, Carbohydr. Res. 70 (1979) 19-25.
[24] A.A. Bothner-By, Geminal and vicinal proton-proton coupling constants in organic compounds, in: J. S. Waugh (Ed.), Advances in Magnetic and Optical Resonance, Vol. 1, Academic Press, Cambridge, 1965, pp.195-316.

https://doi.org/10.30799/jnpr.118.25100201

Cite this Article as: Antonio J. Oliveros-Ortiz, Jessica M. Lorenzo-García, Gabriela Rodríguez-García, Rosa E. del Río, Armando Talavera-Alemán, Mario A. Gómez-Hurtado, Complete ^{1}H NMR assignment of 3-oxo-γ-costic acid from *Ageratina glabrata*, J. Nat. Prod. Resour. 10(2) (2025) 309-315.

Appendix

CONTENTS

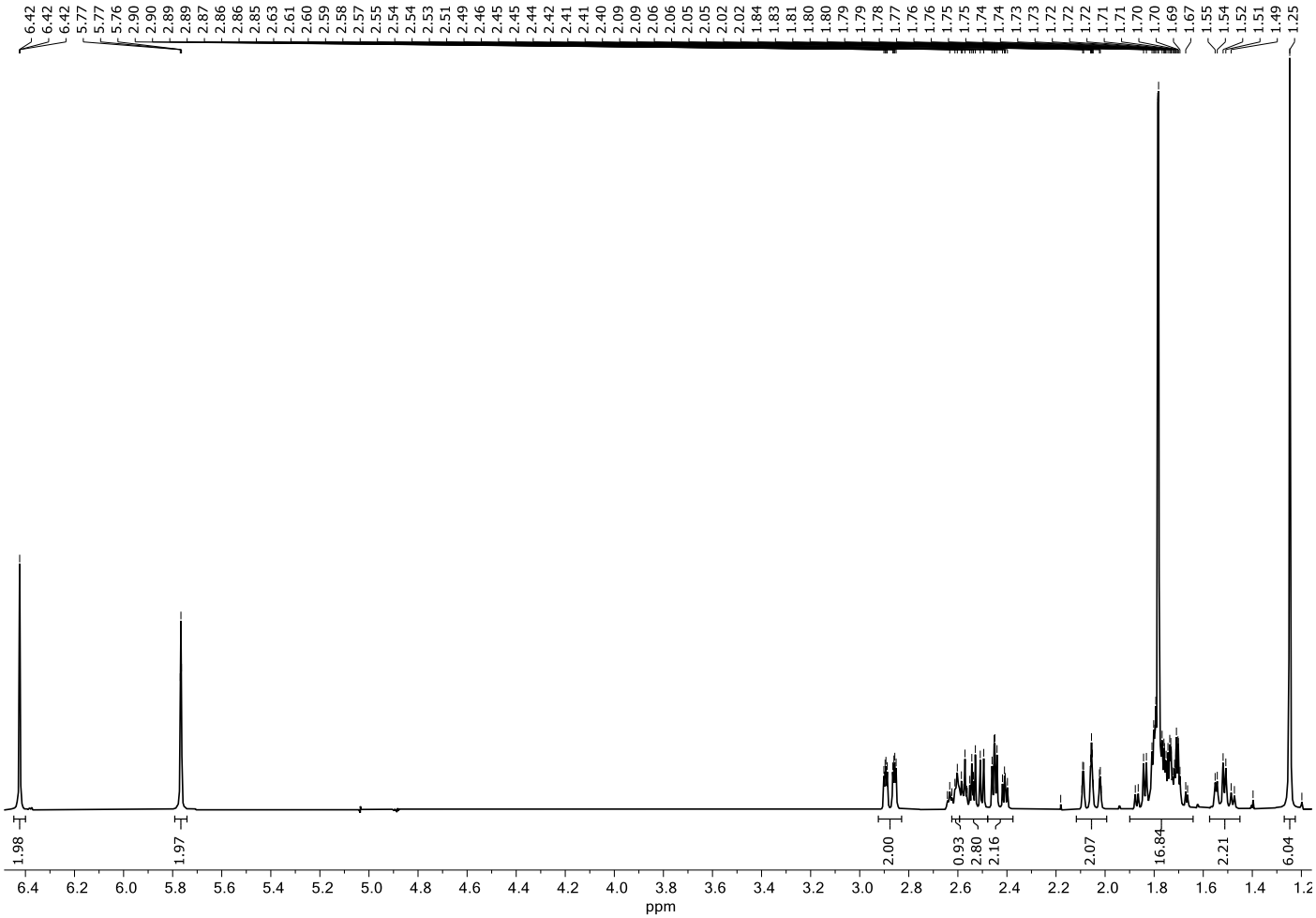

A1. ^{1}H NMR spectrum of 3-oxo-γ-costic acid in $CDCl_3$

https://doi.org/10.30799/jnpr.118.25100201

Cite this Article as: Antonio J. Oliveros-Ortiz, Jessica M. Lorenzo-García, Gabriela Rodríguez-García, Rosa E. del Río, Armando Talavera-Alemán, Mario A. Gómez-Hurtado, Complete ^{1}H NMR assignment of 3-oxo-γ-costic acid from *Ageratina glabrata*, J. Nat. Prod. Resour. 10(2) (2025) 309-315.

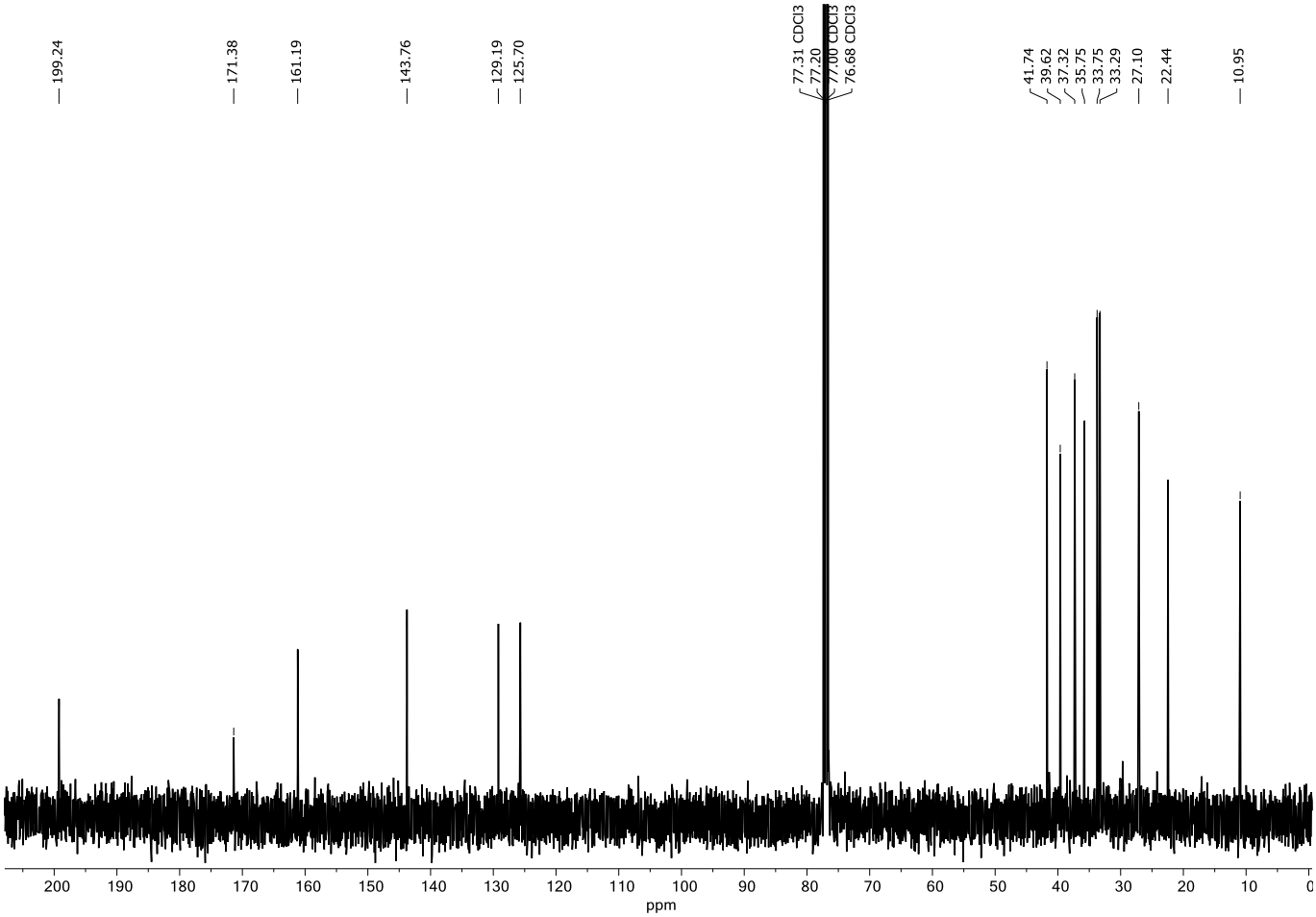

A2. ^{13}C NMR spectrum of 3-oxo-γ-costic acid in $CDCl_3$

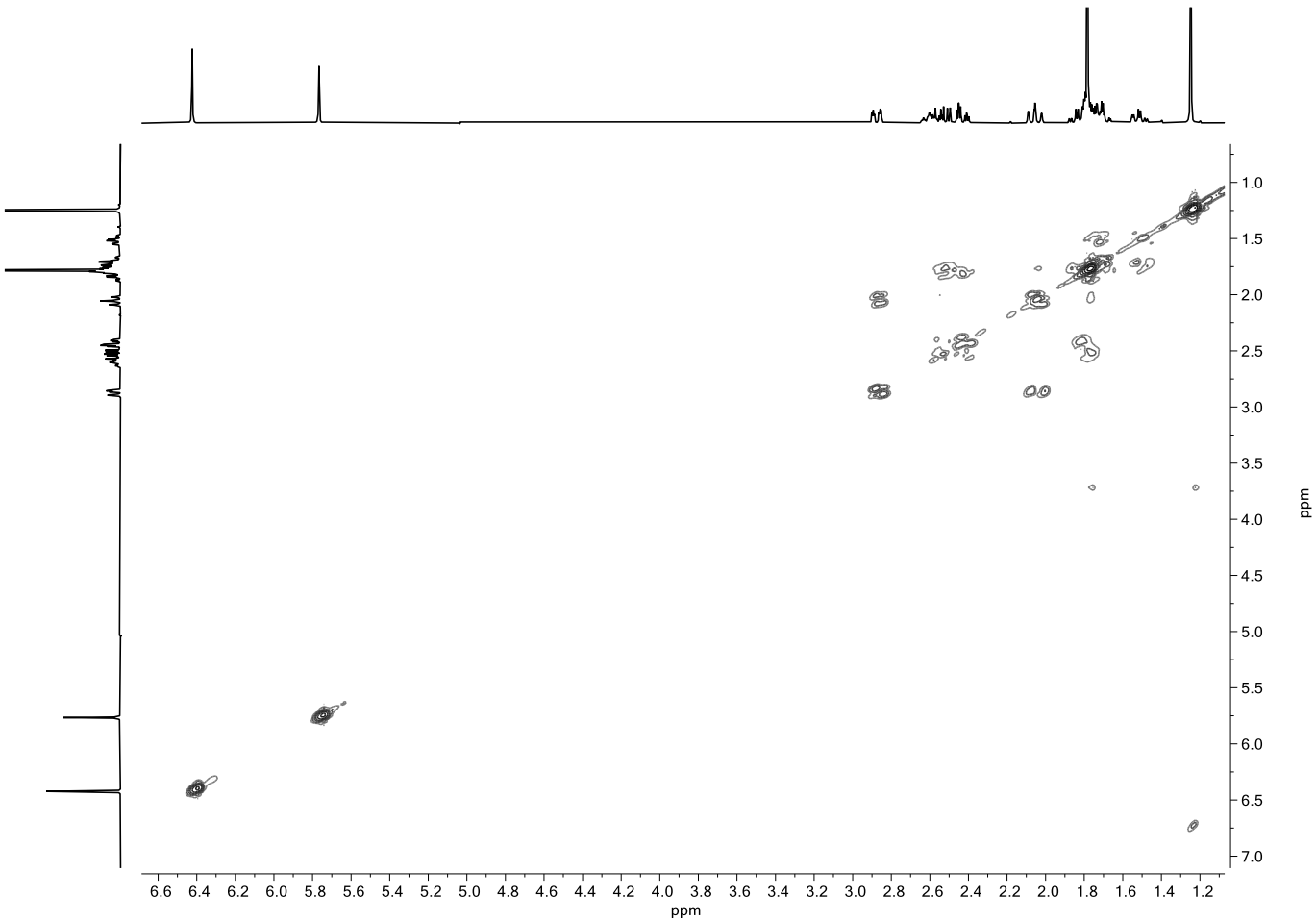

A3. COSY spectrum of 3-oxo-γ-costic acid in $CDCl_3$

https://doi.org/10.30799/jnpr.118.25100201

Cite this Article as: Antonio J. Oliveros-Ortiz, Jessica M. Lorenzo-García, Gabriela Rodríguez-García, Rosa E. del Río, Armando Talavera-Alemán, Mario A. Gómez-Hurtado, Complete ^{1}H NMR assignment of 3-oxo-γ-costic acid from *Ageratina glabrata*, J. Nat. Prod. Resour. 10(2) (2025) 309-315.

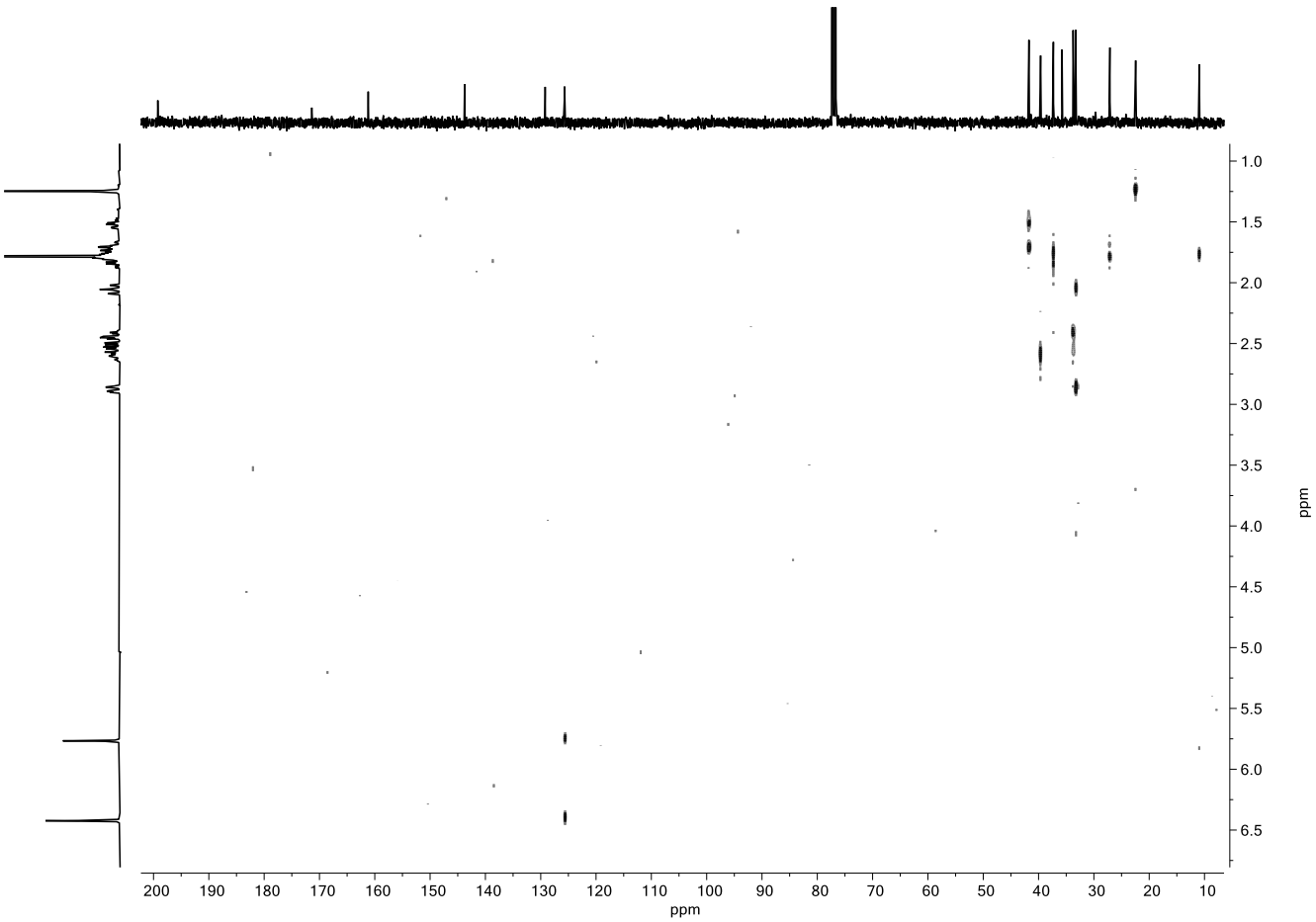

A4. HECTCOR spectrum of 3-oxo-γ-costic acid in $CDCl_3$

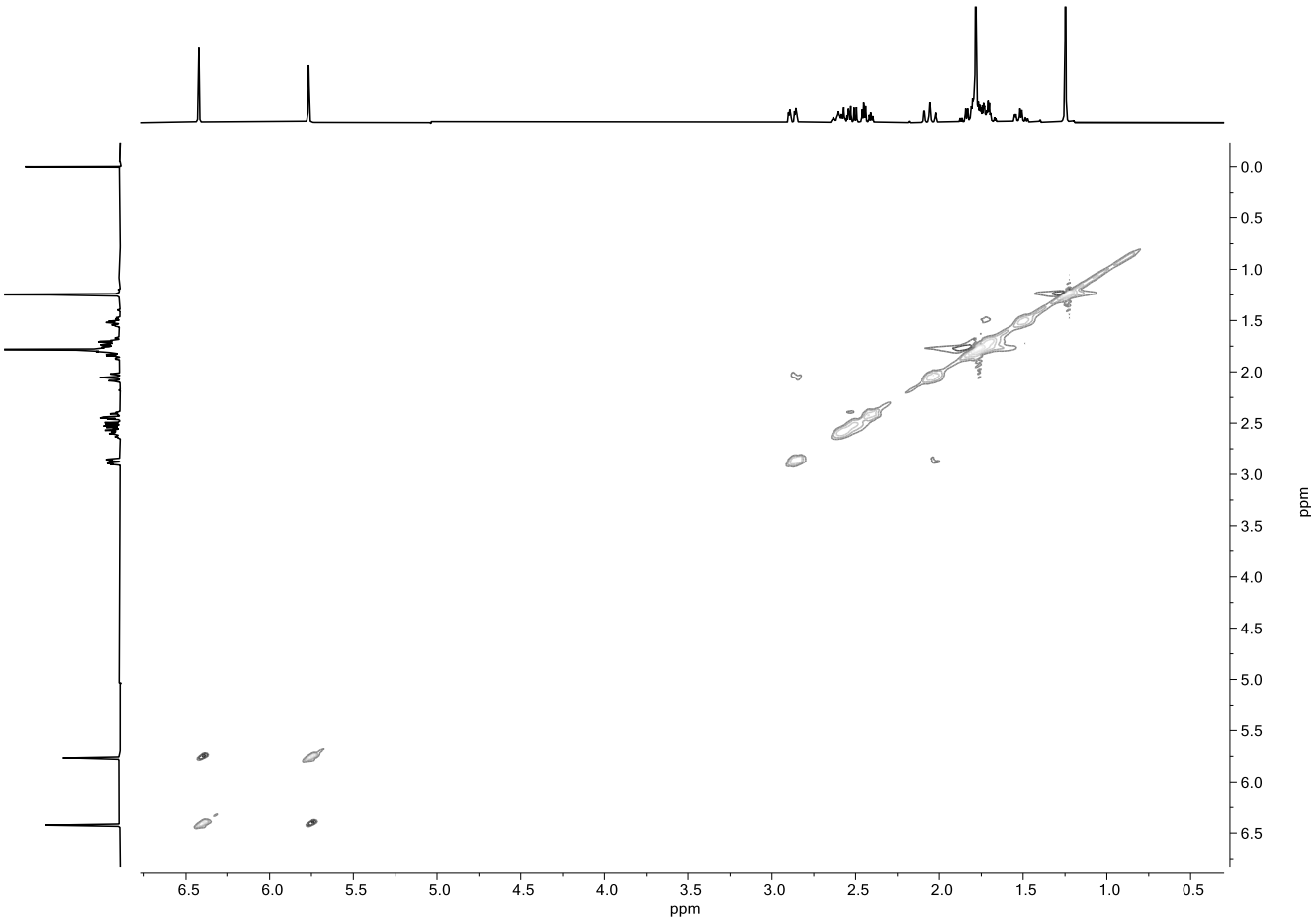

A5. NOESY spectrum of 3-oxo-γ-costic acid in $CDCl_3$

https://doi.org/10.30799/jnpr.118.25100201

Cite this Article as: Antonio J. Oliveros-Ortiz, Jessica M. Lorenzo-García, Gabriela Rodríguez-García, Rosa E. del Río, Armando Talavera-Alemán, Mario A. Gómez-Hurtado, Complete ^{1}H NMR assignment of 3-oxo-γ-costic acid from *Ageratina glabrata*, J. Nat. Prod. Resour. 10(2) (2025) 309-315.

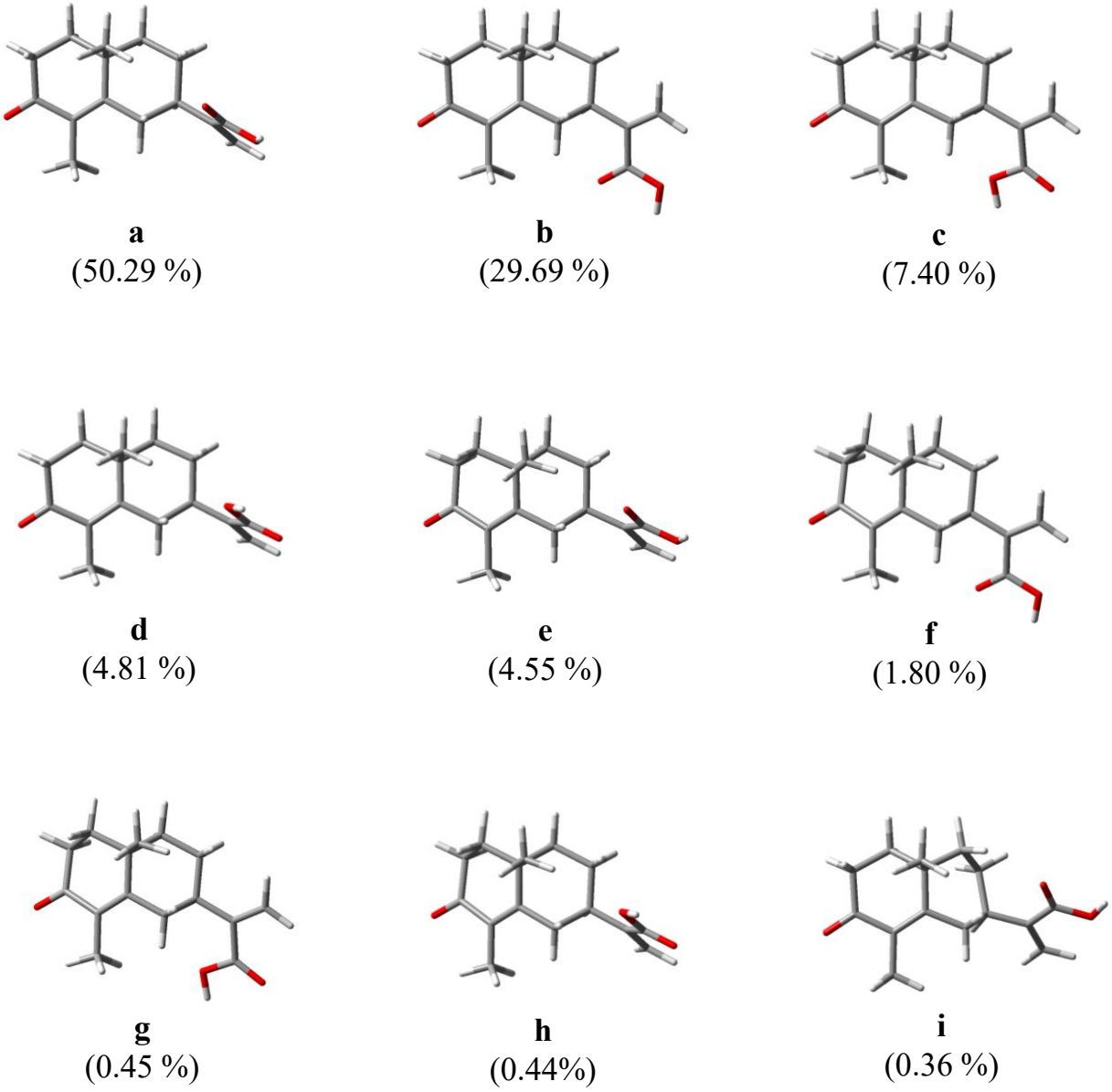

A6. Calculated conformers of 3-oxo-γ-costic acid (**a**-**i**) at the DFT B3LYP/6-31G(d,p) basis set

A7. Thermochemical analysis of 3-oxo-γ-costic acid

Conformer	ΔE_{MMFF}[a]	$\%_{MMFF}$[b]	ΔG_{OPT}[c]	$\%_{OPT}$[d]
a	0.000	0.601	0.000	0.503
b	0.463	0.275	0.312	0.297
c	1.322	0.065	1.134	0.074
d	2.008	0.020	1.389	0.048
e	1.777	0.030	1.421	0.046
f	2.756	0.006	1.972	0.018
g	3.663	0.001	2.789	0.005
h	3.725	0.001	2.809	0.004
i	4.690	0.000	2.930	0.004

[a] Molecular mechanics energies relative to **a** with E_{MMFF} = 15.9725 kcal/mol.
[b] Population in % calculated from the MMFF energies according to $\Delta E_{MMFF} \approx RT \ln K$.
[c] Gibbs free energies relative to **a** for B3LYP/6-31G(d,p)= −507746.04351005645kcal/mol.
[d] Population in % calculated from Gibbs free energies according to $\Delta G = -RT \ln K$.

https://doi.org/10.30799/jnpr.118.25100201

Cite this Article as: Antonio J. Oliveros-Ortiz, Jessica M. Lorenzo-García, Gabriela Rodríguez-García, Rosa E. del Río, Armando Talavera-Alemán, Mario A. Gómez-Hurtado, Complete ^{1}H NMR assignment of 3-oxo-γ-costic acid from *Ageratina glabrata*, J. Nat. Prod. Resour. 10(2) (2025) 309-315.